

Initial- versus final-state effects in the narrow-band spectra of heavy-fermion systems

B. Gumhalter

Institute of Physics of the University of Zagreb, Zagreb, Yugoslavia

V. Zlatić*

Max-Planck-Institut für Festkörperforschung, Stuttgart, Federal Republic of Germany

(Received 22 January 1990; revised manuscript received 5 June 1990)

The f -electron spectral density of heavy-fermion systems, as observed by x-ray photoelectron spectroscopy (XPS) and bremsstrahlung isochromat spectroscopy (BIS), is discussed in terms of initial- and final-state effects. The properties of the initial state, described by the periodic Anderson model, are obtained from the adiabatic perturbation theory, with the on-site correlation U_{ff} taken as the expansion parameter. In the final state the transient effects following the sudden ionization of the system in XPS or BIS are discussed by using the time-dependent perturbation expansion. The overall spectral shapes, as would be observed experimentally, turn out to be given as a convolution of the adiabatic spectral function, which reflects the many-body interactions in the initial state, and the shape function, which accounts for the nonadiabatic effects following the destruction of the charge neutrality in XPS and BIS. Our treatment allows us to explain the position and the shape of the f -derived peaks in the XPS spectra of actinide intermetallics and to remove the conceptual difficulty in understanding the data acquired independently from thermodynamic (low-energy) and spectroscopic (high-energy) measurements of heavy fermions within a unified framework.

I. INTRODUCTION

Many of the unusual properties of heavy-fermion intermetallic compounds can be understood¹ by assuming that the correlated $4f$ states of rare earth or $5f$ states of actinides overlap a broad conduction band of s, p, d symmetry. The hybridization between the atomiclike f states and the neighboring ligand states leads to the formation of the f bands. However, the strong on-site Coulomb interaction between the f electrons of the opposite spin gives rise to many-body effects that make the system behave very differently from what could be expected on the basis of the band-structure calculations in which the local correlations are neglected.

To study these effects we consider a simple model in which the atomiclike f states are represented by orbitally nondegenerate levels located at energy ϵ_f , the conduction electrons are described by a band of width W and of a constant density of states, the hybridization is taken to be due to the off-site hopping, V_{ij} , and the strictly local Coulomb repulsion of the strength U is assumed between f electrons of the opposite spin. In such a model, the interplay between the hybridization and correlation, i.e., the competing tendencies for the f -electron itineracy and localization, leads to the most characteristic feature² of heavy fermion systems: the appearance of two totally different energy scales in the experiments that probe different parts of the electronic spectrum.

At *high energies*, the occupied f -electron states below the Fermi level ϵ_F , resemble the usual single-particle bands of the width $2D$, centered around ϵ_f , i.e., at the position of the singly occupied atomic f states. A similar

structure appears also above ϵ_F , in the unoccupied part of the spectral density, around $\epsilon_f + U$, which corresponds to the doubly occupied atomic level. The relevant energies are defined here on the scale of 1 eV and the observed spectral density has a large weight which accounts for most of the f -derived charge.

At *low energies*, that is, in the vicinity of ϵ_F , the electronic structure³ can be discussed in terms of a narrow "heavy particle band" of the width T_K . The energy spread of such effective "heavy fermion" states is only few meV and their spectral weight is negligibly small. Nonetheless, the presence of this "Kondo peak" in the spectral density gives rise to a large low-temperature mass enhancement and the anomalies in transport and thermodynamic properties of heavy-fermion systems.

Thus, despite the large renormalization of the single-particle spectrum due to the correlations, the electronic properties of heavy fermions in the limit of low ($\epsilon \simeq \epsilon_F$) and high energies ($\epsilon \simeq \epsilon_f$ or $\epsilon \simeq \epsilon_f + U$) can be described by effective f bands, the characteristic energies of which differ by many orders of magnitude ($T_K \ll D$).

The low- and high-energy parts of the f -derived single-particle spectral density are studied most directly by the x-ray photoelectron spectroscopy (XPS) and bremsstrahlung isochromat spectroscopy (BIS) experiments and, in some systems, the two scales discussed above have been observed.⁴ However, the electron removal states and the electron addition states, as measured by XPS and BIS, respectively, are influenced not only by the Coulomb correlation and hybridization, which determine the spectral density of the system unperturbed by the XPS and BIS probes, but also the nonadiabatic final-state

effects that take place whenever the charge neutrality in a nearly localized system is suddenly destroyed by the spectroscopic probe. In both cases the charge equilibrium is destroyed very fast, i.e., in a nonadiabatic fashion, as the electron emission by absorption of a photon in XPS, or the electron injection into an empty state through emission of a photon in BIS, proceeds in a time interval that is much shorter than all other relaxation processes typical of the electron systems considered. In this respect, the electron removal or addition processes may be considered as “sudden” on the time scale characterizing other transitions in the system (which are of the order of W^{-1} , D^{-1} , and T_K^{-1} for the *spd* bands, *f* bands, and the “heavy” bands, respectively).

A sudden removal or addition of an electron in a nearly localized *f*-derived state can be visualized as a creation of an uncompensated charge that will give rise to strong transient localized perturbation acting on the mobile electronic charge in the system, i.e., on the electrons in the conduction band. On the time scale W^{-1} these electrons will respond to such transient perturbation so as to screen out the excess localized charge created in the course of XPS or BIS measurements. The dynamical screening process triggered in this may strongly affect both the position and the shape of the measured *f*-derived density of states, through the final-state relaxation shift and the line shape change, respectively.

In other words, the measured *f* spectra comprise both the initial- (band structure, etc.) and the final-state effects (relaxation shift, peculiar line shape), which are convoluted in a nontrivial manner. Therefore, a comparison between the theory, which accounts solely for the initial band structure, and the experiments, which yield the spectra comprising the initial- as well the final-state effects, become possible only after a careful examination and disentangling of these two groups of features, provided the complexity of the problem allows this at all.

Here, we discuss only the nonadiabatic effects in the XPS and BIS spectra associated with the high-energy *f* states where most of the *f*-electron spectral weight is located. The nonadiabatic effects associated with the “heavy fermion” band, which overlaps ϵ_F and accommodates a negligible fraction of the *f*-electron charge, are here neglected. We should remark also that the heavy fermions in thermal equilibrium exhibit negligibly small *f*-charge fluctuations and their adiabatic properties are well described by the periodic Anderson model, in which the Coulomb coupling between the *f* electrons and the conduction band is neglected. It is only after the sudden creation of the *f* hole by an x-ray that the *f* charge couples to the electron-hole excitations in the conduction band. Since the width of the effective *f* band is much less than the width of the conduction band, i.e., $D \ll W$, the adiabatic calculations for the initial *f*-electron spectral density and the treatment of nonadiabatic corrections, which give rise to the final-state effects, will be performed independently.

The paper is organized as follows. In Sec. II we discuss the electronic structure of heavy fermions described by the periodic Anderson model and show that the adiabatic calculations give the spectral density which has most of

its weight around energies that correspond to the singly and doubly occupied *f* levels, far away from ϵ_F . The imaginary part of the *f*-electron self-energy is here very small and the electronic spectrum can be well described by an effective *f* band of width $2D$ centered around ϵ_f or $\epsilon_f + U$. Taking into account the electron dispersion in this band and the recoil of the XPS created hole, we calculate, in Sec. III, the apparent modifications of the *f* states due to the nonadiabatic effects introduced by suddenly created uncompensated charge. The discussion of our results and the comparison with the experimental data is given in Sec. IV.

II. ADIABATIC CALCULATIONS OF THE SINGLE-PARTICLE SPECTRAL DENSITY

We calculate first, in the adiabatic approximation, the single-particle spectral density for the model Hamiltonian

$$H_a = \sum_{\langle ij \rangle \sigma} t_{ij} c_{i\sigma}^\dagger c_{j\sigma} + \sum_{i\sigma} \epsilon_f f_{i\sigma}^\dagger f_{i\sigma} + \sum_{\langle ij \rangle \sigma} (V_{ij} c_{i\sigma}^\dagger f_{j\sigma} + \text{H.c.}) + U \sum_i n_{i\uparrow} n_{i\downarrow}, \quad (1)$$

where all the symbols have their usual meaning as defined in the Introduction. It has been shown^{5,6} that the qualitative solution to the Hamiltonian (1) can be obtained by the perturbation theory that starts from the normal metallic state and treats U as an expansion parameter. The heavy-fermion features thus obtained are not simply the consequence of the largeness of the Coulomb correlation, but rather the result of an interplay between the correlation and the hybridization effects. Note that already the low-order expansion in powers of U allows, in this approach, an accurate description of the heavy-fermion state.^{5,6}

The *f*-electron spectral density is related to the single-particle Green's function which, in turn, is obtained from the *f*-electron self-energy. To generate the self-energy expansion we rewrite the Hamiltonian (1) by adding and subtracting the Hartree-Fock term, which gives

$$H_a = H_0 + H', \quad (2)$$

where

$$H' = U \sum_i (n_{fi\uparrow} - \langle n_{fi\uparrow} \rangle)(n_{fi\downarrow} - \langle n_{fi\downarrow} \rangle), \quad (3)$$

and where $\langle \rangle_0$ is the grand-ensemble average with respect to the Hartree-Fock Hamiltonian H_0 . We are expanding above the nonmagnetic ground state, so that in the absence of the magnetic field all the quantities we calculate are spin degenerate. The standard *S*-matrix expansion generates the usual diagrams and the expressions thus obtained assume exactly the same form as in the case of the single-impurity Anderson model,⁷ the only difference being that now the momentum conservation supplements the energy conservation at each interaction vertex.

In particular, the reducible *f*-electron self-energy can be written, after Fourier transforming, as⁸

$$\Sigma'_{\mathbf{k}\sigma}(i\Omega_m) = U(\langle\langle n_{i\bar{\sigma}} \rangle\rangle - \langle n_{i\bar{\sigma}} \rangle) + \sum_{n=2}^{\infty} \frac{U^n}{(n-2)!} \frac{1}{N\beta} \prod_{j=1}^n \left[\sum_{l_j=1}^N \int_0^\beta d\tau_j \right] \left\{ \exp[i\mathbf{k}\cdot(\mathbf{R}_{l_1} - \mathbf{R}_{l_n}) - i\omega_m(\tau_1 - \tau_n)] \right. \\ \left. \times D_{1,n}^{n\sigma}(1, \dots, n) D^{n\bar{\sigma}}(1, \dots, n) \right\}_{\text{con}}. \quad (4)$$

Here, $\langle\langle n_{i\bar{\sigma}} \rangle\rangle$ denotes the renormalized f -electron charge, $D^{n\sigma}$ denotes the n th-order determinantal expressions constructed from the Hartree-Fock Green's functions,

$$D^{n\sigma}(1, \dots, n) = \det[(1 - \delta_{ij})G_{ij}^0(\tau_i - \tau_j)],$$

and $D_{1,n}^{n\sigma}$ is the $(n-1)$ -order determinant obtained from $D^{n\sigma}$ by removing its first row and first column. All the other symbols in Eq. (4) have their usual meaning. The only difference between expression (4) and the corresponding expression for the single-impurity problem⁷ is that in addition to the imaginary time integrations, the summation over all the lattice points appears as well.

The unperturbed Green's function and its Fourier transform are defined as

$$G_{i,j\sigma}^0(\tau) = -\langle T_\tau [f_{i\sigma}(\tau) f_{j\sigma}^\dagger(0)] \rangle_0,$$

and

$$G_{\mathbf{k}\sigma}^0(i\Omega_m) = \sum_{ij} \int d\tau G_{ij\sigma}^0(\tau) \exp[-i\mathbf{k}\cdot(\mathbf{R}_i - \mathbf{R}_j) + i\Omega_m \tau] \quad (5)$$

where \sum_{ij} denotes the sum over the lattice sites and $\mathbf{R}_i, \mathbf{R}_j$ are the lattice vectors. From Eqs. (1), (2), and (5), we obtain the unrenormalized quantities:

$$G_{\mathbf{k}\sigma}^0(i\Omega_m) = \frac{\alpha_{\mathbf{k}\sigma}^+}{i\Omega_m - E_{\mathbf{k}\sigma}^+} + \frac{\alpha_{\mathbf{k}\sigma}^-}{i\Omega_m - E_{\mathbf{k}\sigma}^-}, \quad (6)$$

where the coefficients $\alpha_{\mathbf{k}\sigma}^\pm$ and the Hartree-Fock excitation energies $E_{\mathbf{k}\sigma}^\pm$ are given by the expressions

$$\alpha_{\mathbf{k}\sigma}^\pm = 1 \pm \frac{E_f - \epsilon_{\mathbf{k}}}{[(E_f - \epsilon_{\mathbf{k}})^2 + 4V_{\mathbf{k}}^2]^{1/2}} \quad (7)$$

and

$$E_{\mathbf{k}\sigma}^\pm = \frac{1}{2} \{ E_f + \epsilon_{\mathbf{k}} \pm [(E_f - \epsilon_{\mathbf{k}})^2 + 4V_{\mathbf{k}}^2]^{1/2} \} + \mu. \quad (8)$$

Here, $\epsilon_{\mathbf{k}}$, $V_{\mathbf{k}}$, E_f , and μ are the unperturbed energies of the conduction band, the Fourier transform of the hybridization matrix element, the Hartree-Fock position of the f level, and the chemical potential, respectively. Note, that in Eqs. (7) and (8) we should take $E_f = \epsilon_f + U \langle n_{f\sigma} \rangle = 0$ and $\mu = 0$, when discussing the model with the electron-hole symmetry, i.e., $\epsilon_f = -U/2$ and $\langle n_f \rangle = \langle n_c \rangle = 1$.

The renormalized f -electron Green's function can now be written as

$$G_{\mathbf{k}\sigma}(i\Omega_m) = \frac{\tilde{\alpha}_{\mathbf{k}\sigma}^+}{i\Omega_m - \tilde{E}_{\mathbf{k}\sigma}^+} + \frac{\tilde{\alpha}_{\mathbf{k}\sigma}^-}{i\Omega_m - \tilde{E}_{\mathbf{k}\sigma}^-}, \quad (9)$$

where the renormalized coefficients $\tilde{\alpha}_{\mathbf{k}\sigma}^\pm$ and the renormalized excitation energies $\tilde{E}_{\mathbf{k}\sigma}^\pm$ are obtained from the Hartree-Fock expressions (7) and (8) by replacing the Hartree-Fock level E_f by the irreducible self-energy $\Sigma_{\mathbf{k}\sigma}(z)$. The latter is related to the reducible one, $\Sigma'_{\mathbf{k}\sigma}(z)$, as

$$\Sigma_{\mathbf{k}\sigma}(z) = \Sigma'_{\mathbf{k}\sigma}(z) [1 + \Sigma'_{\mathbf{k}\sigma}(z) G_{\mathbf{k}\sigma}(z)]^{-1}. \quad (10)$$

The usefulness of the perturbative approach stems from the fact that the physically relevant results are obtained already with the second-order approximation to Eq. (4), which reads

$$\Sigma_{\mathbf{k}\sigma}(z) = -\frac{U^2 T^2}{N^2} \sum_{\substack{pq \\ \Omega_m \epsilon_n}} G_{\mathbf{k}+\mathbf{p}\sigma}^0(z + i\epsilon_n) G_{\mathbf{q}+\mathbf{p}\sigma}^0(i\Omega_m + i\epsilon_n) \\ \times G_{\mathbf{q}\sigma}^0(i\Omega_m). \quad (11)$$

The frequency summations in Eq. (11) are easily performed⁹ but the momentum integrations have to be performed numerically even for the one-dimensional lattices.

However, if we restrict our considerations to the energies around ϵ_f or $\epsilon_f + U$ only, which are relevant for the XPS and BIS experiments, respectively, $\Sigma_{\mathbf{k}\sigma}(z)$ can be obtained analytically. In the symmetric model and for $U \gg |V_{\mathbf{k}}^2|^{1/2}$ we have $[-\epsilon_f, \epsilon_f + U] \gg |V_{\mathbf{k}}^2|^{1/2}$, so that the self-energy expression (11) becomes

$$\Sigma_{\mathbf{k}\sigma}(\epsilon + i\delta) = \frac{U^2}{N^2} \sum_{pq} \alpha_{\mathbf{p}\sigma}^- \alpha_{\mathbf{p}+\mathbf{k}\sigma}^+ (\alpha_{\mathbf{k}+\mathbf{q}\sigma}^+ + \alpha_{\mathbf{k}+\mathbf{q}\sigma}^-) \frac{1}{\epsilon + i\delta}, \quad (12)$$

which, using the properties of the coefficients $\alpha_{\mathbf{p}\sigma}^-$ and $\alpha_{\mathbf{p}\sigma}^+$, simplifies to⁵

$$\Sigma_{\mathbf{k}\sigma}(\epsilon + i\delta) = \frac{U^2/4}{\epsilon + i\delta}. \quad (13)$$

Thus, at high energies the self-energy can be very well approximated by a local \mathbf{k} -independent quantity so that $G_{\mathbf{k}\sigma}$ acquires simple poles around ϵ_f and $\epsilon_f + U$. This further implies the occurrence of two prominent f -derived peaks or bands in the density of f states.

To obtain detailed features of the f -electron spectral density we have to use the full self-energy, Eq. (11), and evaluate the expression

$$N_f^\sigma(\epsilon) = -\frac{2}{\pi} \sum_{\mathbf{k}} \text{Im} G_{\mathbf{k}\sigma}(\epsilon + i\delta), \quad (14)$$

where $G_{\mathbf{k}\sigma}(\epsilon + i\delta)$ is the analytic continuation of $G_{\mathbf{k}\sigma}(z)$ onto the real axis, the summation over \mathbf{k} runs over the first Brillouin zone, and the factor of 2 is the result of the

spin degeneracy. The numerical analysis shows^{2,6,10} that in the Kondo limit and at $T=0$ K the f -electron spectral density displays two energy scales: (i) the Kondo peak of small spectral weight appears at ε_F , the characteristic energy being set by the Kondo temperature T_K ; (ii) most of the spectral weight is associated with two broad peaks centered at ε_f and $\varepsilon_f + U$, and the characteristic energy scale is defined by $D \simeq \langle V^2 \rangle / W$. Here, we take the parameters such that $-\varepsilon_f = U/2 \simeq 3-5$ eV and thereby obtain $D \simeq 1-2$ eV. As regards the finite-temperature effects, the many-body peak at ε_F is strongly temperature dependent and disappears above the Kondo temperature, while the peaks at ε_f and $\varepsilon_f + U$ do not change much as the temperature varies between the room temperature and $T=0$ K. Furthermore, it turns out that the high-energy structure of the adiabatic spectral density is very well described by the local approximation, which gives the density of states shown in Fig. 1.

The high-energy part of the excitation spectrum, determined from the transcendental equation $[\varepsilon - \bar{E}_{f\mathbf{k}}(\varepsilon)] = 0$, can be approximated by an effective f band of width $2D$ and dispersion $\bar{\varepsilon}_{f\mathbf{k}}$. In particular, the analysis of the one-dimensional periodic Anderson model with linear dispersion,

$$\varepsilon_{f\mathbf{k}} = \varepsilon_F + \{ [2W/(\pi/d)]k - W \} ,$$

in the unperturbed conduction band and with the hybridization taken as $V_{\mathbf{k}}^2 = V^2[1 - (\varepsilon_{\mathbf{k}}/W)^2]$, shows⁹ that in a narrow energy range around ε_f the renormalized f states will assume dispersion

$$\bar{\varepsilon}_{f\mathbf{k}} = \varepsilon_f + \{ [2D/(\pi/d)]k - D \} .$$

A quasiparticle band of similar structure appears around $\varepsilon_f + U$ as well. This further implies that within an energy interval $\simeq D$ around the energies ε_f and $\varepsilon_f + U$, the wave vector \mathbf{k} remains a good quantum number even for the description of the strongly renormalized f states. This feature of the present model will be largely exploited in the discussion of the nonadiabatic or transient effects that

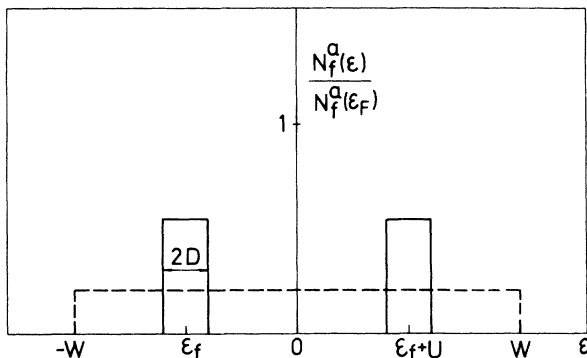


FIG. 1. Sketch of the high-energy part of the f -derived density of states, $N_f^a(\varepsilon)/N_f^a(\varepsilon_F)$ evaluated in the local approximation and plotted as a function of energy ($\varepsilon_F=0$) for $U/W=1$, $W/D=10$, and $\varepsilon_f = -U/2$ (solid line). Unperturbed spd band is shown for comparison (dashed line).

occur in the high-energy parts of the electronic density of states as probed by the XPS and BIS measurements.

III. NONADIABATIC EFFECTS IN THE XPS AND BIS SPECTRA

A. Formulation of the problem of nonadiabaticity

In the XPS or BIS of localized or nearly localized electronic states one suddenly destroys the local charge equilibrium by emission or addition of one electron in an f state, which leads to the appearance of the final-state effects in the measured spectra. In one of the previous works¹¹ we have studied the role of the nonadiabaticity in heavy-fermion systems by assuming incoherent f states. Here, we extend our studies of these effects also to the systems in which the f states are broadened into narrow bands lying well below or above the Fermi level which itself is located in the s, p, d continuum (see Fig. 1).

A convenient approach to treat the initial- and final-state effects in the spectral density of f -derived states of heavy-fermion systems is to extend the Hamiltonian (1), which describes the initial-state effects only, by a term that would account for the coupling of the uncompensated final-state f charge (a hole in the occupied f -derived band around ε_f in XPS or an electron in the empty band around $\varepsilon_f + U$ in BIS), with the conduction electrons near the Fermi level, viz., with the charge-density fluctuations within the occupied s, p, d band.

In a Fermion system the charge-density fluctuations or electron-hole excitations near the Fermi level can be modeled, to a good approximation in most cases of practical interest, by the bosonized electron-hole pairs that are characterized by their excitation energy ν and wave vector \mathbf{q} . With this in mind, we shall reduce the problem of the interaction of the XPS- or BIS-induced excess charge in the f -derived bands with the electrons in the conduction band of the system to a problem of the interaction of the excess charge with the bosonized excitations of the conduction band.

To this end, we introduce the bosonic creation and annihilation operators $a_{\mathbf{q}\nu}^\dagger$ and $a_{\mathbf{q}\nu}$, respectively, through the following commutation rules:¹²

$$[a_{\mathbf{q}\nu}, a_{\mathbf{q}'\nu'}^\dagger] = \frac{\delta_{\mathbf{q},\mathbf{q}'} \delta(\nu - \nu')}{S_{\mathbf{q}}(\nu)} , \quad (15)$$

where $S_{\mathbf{q}}(\nu)$ is the density of electron-hole excitations per unit energy interval or the dynamic form factor pertinent to the conduction electrons [e.g., Lindhard function if the response of the conduction-band electrons is treated within the random-phase approximation [(RPA)]. Remembering that \mathbf{k} remains a good quantum number for f electrons in the interval around ε_f and $\varepsilon_f + U$, we may write for the nonadiabatic or transient part of the total Hamiltonian:

$$H_{\text{trans}}^{\text{BIS}} = \sum_{\mathbf{k}, \mathbf{q}\nu} V_{\mathbf{k}\mathbf{k}-\mathbf{q}} f_{\mathbf{k}-\mathbf{q}}^\dagger f_{\mathbf{k}} (a_{\mathbf{q}\nu} + a_{-\mathbf{q}\nu}^\dagger) , \quad (16)$$

in the case of the interaction of a BIS-promoted f -electron with the conduction band, and

$$H_{\text{trans}}^{\text{XPS}} = \sum_{\mathbf{k}, \mathbf{q}\nu} V_{\mathbf{k}-\mathbf{q}\mathbf{k}} f_{\mathbf{k}-\mathbf{q}} f_{\mathbf{k}}^{\dagger} (a_{\mathbf{q}\nu} + a_{-\mathbf{q}\nu}^{\dagger}), \quad (17)$$

in the case of the interaction of an XPS-created hole in the f band with the conduction electrons. In both expressions (16) and (17) the matrix element of the Coulomb interaction U_{fc} between the f charge and the conduction electrons is given by

$$U_{fc} = \langle \mathbf{k}-\mathbf{q} | V(r) | \mathbf{k} \rangle = V_{\mathbf{k}-\mathbf{q}\mathbf{k}}, \quad (18)$$

where $V(r) = -e^2/r$ (not to be confused with the f - s, p, d hybridization potential), and the summation over ν must be carried out in accordance with (15) as

$$\sum_{\nu} \rightarrow \int_0^{\infty} d\nu S_{\mathbf{q}}(\nu). \quad (19)$$

Also, in order to preserve the formal consistency of our approach, the total Hamiltonian has to be extended by the "adiabatic" free-boson term

$$H_{\text{boson}}^0 = \sum_{\mathbf{q}\nu} \nu a_{\mathbf{q}\nu}^{\dagger} a_{\mathbf{q}\nu}, \quad (20)$$

although the latter should not be taken into account in the calculations of the initial-state, adiabatic properties of the system. Hence, the full Hamiltonian that describes the dynamics of the heavy-fermion system, including the nonadiabatic effects, now reads

$$H = H_a + H_{\text{boson}}^0 + H_{\text{trans}}, \quad (21)$$

where H_a is given by Eq. (1). Here, and in what follows, the spin index is omitted, while the quantities corresponding to the adiabatic part of the problem are labeled accordingly.

In the following discussion we shall consider only the dynamic relaxation processes consecutive to the XPS creation of a hole in the occupied part of the f -derived band around ϵ_f . The treatment of the processes following the sudden promotion of a BIS electron into the f -derived empty band around $\epsilon_f + U$, can be obtained simply by time reversal.¹³

An important property of the interaction (17) is that it becomes effective only if there exists a photocreated hole in the otherwise occupied f -derived band. Namely, due to the large separation of the center of this band from the Fermi level (i.e., $U \gg D$), we may altogether neglect the virtual excitations of the f hole created by x-ray absorption. This allows us to reduce the problem to the one in which there is only a single hole present in the f band at any instant, which in the language of propagators, means that the hole propagates in one time direction only.

The density of states of the occupied f band $N_f(\omega)$, which now comprises both the initial- and final-state effects, as measured by XPS, is obtained at $T=0$ from the standard expression

$$\begin{aligned} N_f(\omega) &= 2 \sum_{\mathbf{k}} N_{f\mathbf{k}}(\omega) = \frac{2}{\pi} \sum_{\mathbf{k}} \text{Im} G_{\mathbf{k}}(\omega) \\ &= \frac{2}{\pi} \text{Im Tr} G(\omega - i\delta), \end{aligned} \quad (22)$$

in which the trace has to be taken only over the \mathbf{k} states within the f band. The diagonal elements $G_{\mathbf{k}}(\omega)$, which appear in the expression, are obtained from the Fourier transform of the diagonal f -state Green's function calculated in the presence of $H_{\text{trans}}^{\text{XPS}}$, viz.,

$$G_{\mathbf{k}}(\omega) = \int_{-\infty}^{\infty} dt \exp(i\omega t) G_{\mathbf{k}}(t), \quad (23)$$

with $G_{\mathbf{k}}(t)$ now defined as

$$G_{\mathbf{k}}(t) = -i \langle 0 | T [f_{\mathbf{k}}(t) f_{\mathbf{k}}^{\dagger}(0)] | 0 \rangle. \quad (24)$$

Here, $|0\rangle$ denotes the ground state of the heavy-fermion system before the hole has been created in x-ray photoemission, i.e., before H_{trans} has become effective. Hence, $|0\rangle$ is an eigenstate of the adiabatic part H_a of the total Hamiltonian H given by (21), which incorporates all the initial-state effects brought about by the f - spd hybridization $V_{\mathbf{k}}$ and the Anderson correlation U . Since we are allowing for the presence of only one f hole at any instant in the system, Eq. (24) can be brought to the form

$$\begin{aligned} G_{\mathbf{k}}(t) &= i\Theta(-t) \langle 0 | f_{\mathbf{k}}^{\dagger}(0) f_{\mathbf{k}}(t) | 0 \rangle \\ &= i\Theta(-t) \langle 0 | f_{\mathbf{k}}^{\dagger} e^{iHt} f_{\mathbf{k}} e^{-iHt} | 0 \rangle \\ &= i\Theta(-t) \langle 0 | f_{\mathbf{k}}^{\dagger} e^{iHt} f_{\mathbf{k}} e^{-iH_a t} | 0 \rangle \\ &= i\Theta(-t) e^{-iE_0^a t} \langle 0_{f\mathbf{k}} | e^{iHt} | 0_{f\mathbf{k}} \rangle, \end{aligned} \quad (25)$$

where $|0_{f\mathbf{k}}\rangle$ denotes the eigenstate of H_a with one hole present in the \mathbf{k} state of the f band. In deriving the last line of Eq. (25), we have made use of the fact that

$$H|0\rangle = H_a|0\rangle = E_0^a|0\rangle, \quad (26)$$

since on the time scale set by H_{trans} ($\tau \sim W^{-1}$) the ground-state fluctuations of the f hole can be neglected. The expression (25) enables us to represent the diagonal single-hole propagator by the expectation value of the evolution operator $\exp(iHt)$ in an excited state $|0_{f\mathbf{k}}\rangle$ of the heavy-fermion system. Here we recall that the diagonal matrix elements of the evolution operator can be most conveniently obtained by employing the cumulant expansion or by writing

$$\begin{aligned} \langle 0_{f\mathbf{k}} | e^{iHt} | 0_{f\mathbf{k}} \rangle &= \langle 0_{f\mathbf{k}} | e^{iH_a t} T \exp \left[i \int_0^t d\tau H_{\text{trans}}^I(\tau) \right] | 0_{f\mathbf{k}} \rangle \\ &= e^{iE_{f\mathbf{k}}^a t} \langle 0_{f\mathbf{k}} | T \exp \left[i \int_0^t d\tau H_{\text{trans}}^I(\tau) \right] | 0_{f\mathbf{k}} \rangle, \end{aligned} \quad (27)$$

where $H_{\text{trans}}^I(\tau)$ is written in the interaction representation, defined here as

$$H_{\text{trans}}^I(\tau) = e^{-iH_a \tau} H_{\text{trans}} e^{iH_a \tau} \quad (28)$$

and

$$H_a |0_{f\mathbf{k}}\rangle = E_{f\mathbf{k}}^a |0_{f\mathbf{k}}\rangle = (E_0^a - \bar{\epsilon}_{f\mathbf{k}}) |0_{f\mathbf{k}}\rangle, \quad (29)$$

where

$$\bar{\epsilon}_{f\mathbf{k}} = E_0^a - E_{f\mathbf{k}}^a \quad (30)$$

is the energy of an electron in state $|\mathbf{k}\rangle$.

Now, combining (25) and (29), we finally obtain

$$\begin{aligned} G_{\mathbf{k}}(t) &= i\Theta(-t)e^{-i\tilde{\epsilon}_{f\mathbf{k}}t}e^{C_{f\mathbf{k}}(t)} \\ &= G_{\mathbf{k}}^a(t)e^{C_{f\mathbf{k}}(t)}, \end{aligned} \quad (31)$$

where $G_{\mathbf{k}}^a(t)$ is the renormalized zero-temperature f -hole Green's function pertinent to the adiabatic Hamiltonian (1) and $C_{f\mathbf{k}}(t)$ stands for the expectation value of the T -ordered exponential, which has a power expansion in powers of the coupling constant (i.e., $V_{\mathbf{k}-\mathbf{q}\mathbf{k}}$), starting from the second order.^{14,17} In the following we shall restrict ourselves to the second-order term in the expansion for $C_{f\mathbf{k}}(t)$, which amounts to describing the phase shift pertinent to the scattering potential $V_{\mathbf{k}-\mathbf{q}\mathbf{k}}$ in the Born approximation. In this case we obtain^{15,16}

$$C_{f\mathbf{k}}(t) = - \int_{-\infty}^{\infty} d\omega' \rho_{f\mathbf{k}}(\omega') \frac{1 - e^{i\omega't + i\omega't}}{(\omega')^2}, \quad (32)$$

where¹⁷

$$\rho_{f\mathbf{k}}(\omega') = \sum_{\mathbf{q}} |V_{\mathbf{k}-\mathbf{q}\mathbf{k}}|^2 \int_0^{\infty} d\nu S_{\mathbf{q}}(\nu) \delta(\omega' - \nu + \tilde{\epsilon}_{f\mathbf{k}-\mathbf{q}} - \tilde{\epsilon}_{f\mathbf{k}}) \quad (33)$$

is the weighted density of excitations characteristic of the composite system (single f -hole+electron-hole pair in the conduction band). An important feature of expression (33) is that it encompasses the recoil of the f hole upon exciting a conduction electron-hole pair of wave vector \mathbf{q} and energy ν . These recoil effects enter $\rho_{f\mathbf{k}}(\omega')$ through the interaction matrix element $V_{\mathbf{k}-\mathbf{q}\mathbf{k}}$ and the recoil energy of the f hole

$$\Delta_{\mathbf{k}\mathbf{q}} = \tilde{\epsilon}_{f\mathbf{k}-\mathbf{q}} - \tilde{\epsilon}_{f\mathbf{k}}. \quad (34)$$

In the case of an infinitely heavy hole one has $\Delta_{\mathbf{k}\mathbf{q}}=0$ and this may enable the factorization of the \mathbf{q} and ν integrations in (33), provided the same property also holds for $S_{\mathbf{q}}(\nu)$. The expression (32) can be also represented by and derived from the Feynman diagrams in the (\mathbf{k}, t) space (cf. Ref. 15). However, the $V_{\mathbf{k}-\mathbf{q}\mathbf{k}}$ vertices in these diagrams are restricted to the time interval $(0, t)$ during which H_{trans} in (27) is effective (cf. Refs. 16, 19, and 21). This is in contrast to the ordinary diagrams appearing in the treatment of the adiabatic properties of the system described by H_a , the vertices of the latter being effective within the entire time interval $(-\infty, \infty)$.

The expressions (23)–(32) enable us now to write the f -band density of states (22) in a compact form:

$$\begin{aligned} N_f(\omega) &= 2 \sum_{\mathbf{k}} \int_{-\infty}^{\infty} \frac{dt}{2\pi} e^{i(\omega - \tilde{\epsilon}_{f\mathbf{k}})t + C_{f\mathbf{k}}(t)} \\ &= \sum_{\mathbf{k}} \int_{-\infty}^{\infty} d\omega' N_{f\mathbf{k}}^a(\omega') N_{f\mathbf{k}}^{\text{trans}}(\omega - \omega'), \end{aligned} \quad (35)$$

where

$$N_{f\mathbf{k}}^a(\omega) = \frac{2}{\pi} \text{Im} G_{\mathbf{k}}^a(\omega - i\delta)$$

is the effective density of f states in the absence of H_{trans} . On the other hand, the shape function

$$N_{f\mathbf{k}}^{\text{trans}}(\omega') = \int_{-\infty}^{\infty} \frac{dt}{2\pi} e^{i\omega't + C_{f\mathbf{k}}(t)} \quad (36)$$

describes the final-state relaxation processes brought about by the sudden switching on of H_{trans} in XPS measurements, and as such introduces the final-state effects into the total measured spectral density $N_f(\omega)$ of Eq. (35). The remainder of this section will be devoted to model calculations of $N_{f\mathbf{k}}^{\text{trans}}(\omega)$.

B. Model calculations of the shape function

The calculation of the shape function $N_{f\mathbf{k}}^{\text{trans}}(\omega)$ as given by (36) reduces to the calculation of the exponent $C_{f\mathbf{k}}(t)$ defined by Eq. (32). The evaluation of the latter quantity requires the knowledge of the matrix element $V_{\mathbf{k}-\mathbf{q}\mathbf{k}}$ (19), the dynamical form factor $S_{\mathbf{q}}(\nu)$, and the f -hole energy $\Delta_{\mathbf{k}\mathbf{q}}$ (34). However, the present knowledge of the static electronic structure of the heavy-fermion systems does not enable us to go beyond the relatively simple models in describing the *dynamical* properties of these systems. On the other hand, it turns out that some dynamical properties of Fermi liquids in general, and the heavy-fermion systems in particular, depend to a large extent only on quite general parameters and structure of fermionic systems. Hence, in our discussion and the evaluation of the shape function, we shall employ relatively simple-model expressions for the quantities $V_{\mathbf{k}-\mathbf{q}\mathbf{k}}$, $S_{\mathbf{q}}(\nu)$, and $\Delta_{\mathbf{k}\mathbf{q}}$. Thus, for the matrix element of the f -hole conduction-electron Coulomb attraction, we take the expression for the bare interaction,

$$V_{\mathbf{k}-\mathbf{q}\mathbf{k}} = \frac{4\pi e^2}{q^2}, \quad (37)$$

since the screening of this interaction will enter through the self-consistent $S_{\mathbf{q}}(\nu)$. The screening properties of the conduction electrons will be described through an RPA expression for $S_{\mathbf{q}}(\nu)$, corresponding to an electron gas of a given density. Such dynamic form factor comprises electron-hole pairs in the low-energy part of the spectrum $\nu < qv_F$ (where v_F is the Fermi velocity), and the plasmon of frequency ω_p in the high-energy part of the spectrum. While the former type of excitations are always the well-defined constituents of the excitation spectra of normal Fermi liquids, the latter are usually blurred and damped by other electronic transitions appearing in real systems, such as interband transitions, etc. (cf. Fig. 2 of Ref. 18). Hence, in the following we shall take into account only the incoherent electron-hole component of the spectrum $S_{\mathbf{q}}(\nu)$ modeled by the Lindhard function, as it is precisely this part of the spectrum that will most affect the shape function (see below). Thus, we take¹⁹

$$S_{\mathbf{q}}(\nu) = \frac{a_q \nu}{q} e^{(-\nu/v_c)} \Theta(\nu) \Theta(2q_F - q), \quad (38)$$

where we have introduced an exponential cutoff $v_c = W$ instead of a sharp one for later mathematical convenience, and

$$a_q \cong \frac{\beta_q^2}{8\pi e^2 v_F}, \quad (39)$$

where β_q is given by

$$\beta_q = \frac{q_{TF}}{|\epsilon(q, \omega \rightarrow 0)|} = \frac{q_{TF}}{1 + q_{TF}^2/q^2},$$

with q_{TF} being the Thomas-Fermi wave vector.

The main effect of the recoil energy Δ_{kq} is to change the volume of the phase space in which the energy conservation is satisfied during the excitation of a conduction-band electron-hole pair through the Coulomb interaction with the photocreated f hole. The very appearance of the recoil in the argument of the δ function on the right-hand side (RHS) of (33) is significant insofar as $\Delta_{kq} \neq 0$, as this gives rise to the nonzero values of $\rho_{fk}(\omega')$ in a certain interval below $\omega' = 0$ [otherwise $\rho_{fk}(\omega' < 0) = 0$ for $\Delta_{kq} = 0$]. Because of this, we shall employ the functional form of Δ_{kq} emerging from the periodic Anderson model described in Sec. II, and treated in the local approximation, which yields

$$\Delta_{kq} = \bar{\epsilon}_{fk-q} - \bar{\epsilon}_{fk} = bq = \frac{2D}{\pi/d} q, \quad (40)$$

where D was defined in Sec. I. The qualitative predictions for the spectral shapes based on such recoil model are the same as for the recoil of free particles (cf. Sec. IV of Ref. 15). A similar model has also been employed in other studies of the interaction of fermions with bosons (cf. Ref. 20, p. 305). Taking this form of the recoil and fixing the parameters appearing in V_{k-qk} , $S_q(\nu)$, and Δ_{kq} , we find that in the present model $\rho_{fk}(\omega')$ is \mathbf{k} independent and exhibits the behavior sketched in Fig. 2 for various values of the dimensionless parameter $a = 2d/bq_{TF} = \pi/dq_{TF}$ and $\gamma = W/D = 5$. Here, small values of q_{TF} (i.e., large a) signify the limit of the f -hole interaction with dense electron gas in the conduction band (large screening effects), and vice versa. The main feature to be observed in Fig. 2 is a power-law dependence of $\rho_{fk}(\omega')$ on ω' near its band bottom, where the latter is obtained

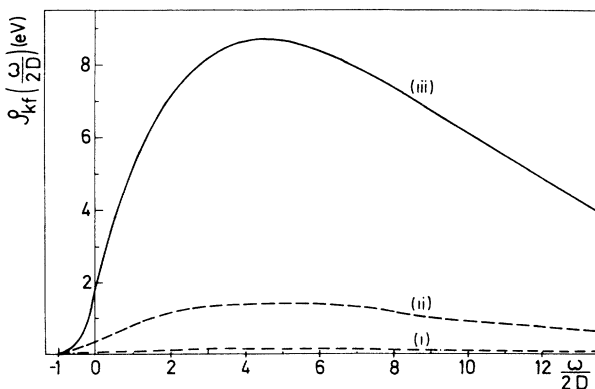


FIG. 2. Density of excitations of the composite system (f -hole + electron-hole pair in the conduction band), $\rho_{fk}(\omega)$, plotted as a function of ω' for $\gamma = W/D = 5$ and various values of the parameters $a = (\pi/d)/q_{TF}$: (i) $a = 0.5$, (ii) $a = 1$, (iii) $a = 2$.

by putting the hole at the lower edge of the filled f band, i.e., for $(\Delta_{kq})_{\max} = 2D$. Then, $\rho_{fk}(\omega')$ rises up linearly with ω' , crosses the $\omega' = 0$ axis, and eventually saturates and falls off because of the presence of the cutoff in $S_q(\nu)$. In the case of an infinitely heavy hole ($M_f \rightarrow \infty \Rightarrow \Delta_{kq} \rightarrow 0$), $\rho_{fk}(\omega')$ starts linearly from zero without exhibiting the power-law behavior, because the latter is exclusively a consequence of the nonvanishing recoil of the f hole (cf. Refs. 15 and 16). The linear low-energy behavior of $\rho_{fk}(\omega')$ is also obtained in a special case if the hole is created at the upper band edge of a filled f band.

The knowledge of $\rho_{fk}(\omega')$ enables us to deduce the general behavior of $C_{fk}(t)$ and thereby of $N_{fk}^{\text{trans}}(\omega)$ as well. Thus, according to (32) we may write

$$C_{fk}(t) = C_{fk}^a(t) + C_{fk}^{\text{trans}}(t), \quad (41)$$

in which the “adiabatic” part linear in t reads

$$C_{fk}^a(t) = -i \left[\int d\omega' \frac{\rho_{fk}(\omega')}{\omega'} \right] t = -iv_f t, \quad (42)$$

where v_f describes the screening energy or the relaxation shift of the f hole created in a state $|\mathbf{k}\rangle$ and interacting with the conduction-band electrons. The term $\exp[C_{fk}^a(t)]$ can now be associated with the unperturbed hole propagator $G_{\mathbf{k}}^a$ in Eq. (30) to yield the relaxed (or shifted) energy of the f hole

$$\bar{\epsilon}_{\mathbf{k}} = \bar{\epsilon}_{f\mathbf{k}} + v_f. \quad (43)$$

The magnitude of v_f depends to some extent on the magnitude of the maximum of $\rho_{fk}(\omega')$, but more important is the position of the maximum with respect to the point $\omega' = 0$ and the extension of the integral in (42) on both sides from this point. Hence, for relatively broad f bands (i.e., $D \sim W$) and $\rho_{fk}(\omega')$ centered around $\omega' = 0$, the contribution to the integral in (42) will be negligibly small. This indicates the absence of any appreciable relaxation due to screening in the case of light or mobile holes. On the other hand, in the case of an infinite f -hole mass ($D = 0$), we have $\Delta_{kq} = 0$ and hence the lower integration boundary in (42) is zero, giving the maximum value of the relaxation shift for a localized hole.

The time dependence of the remainder on the RHS of (41), viz.,

$$C_{fk}^{\text{trans}}(t) = - \int d\omega' \rho_{fk}(\omega') \frac{1 - e^{i\omega't}}{(\omega')^2}, \quad (44)$$

determines the shape function (36) and can be inferred by studying the long- and the intermediate-time dependence of the integral in (44), giving, respectively, the properties of the elastic line at $\omega \simeq \bar{\epsilon}_{\mathbf{k}}$ and the inelastic wing of the f -hole spectrum $N_{fk}(\omega)$ [Eq. (22)], or equivalently, of $N_{fk}^{\text{trans}}(\omega)$ [Eq. (36)].

1. Long-time behavior of $G_{\mathbf{k}}(t)$

To determine the long-time behavior of $C_{fk}^{\text{trans}}(t)$, and thereby of $G_{\mathbf{k}}(t)$, we shall write the integral in (44) in the form

$$\begin{aligned} \lim_{|t| \rightarrow \infty} \int d\omega' \rho_{f\mathbf{k}}(\omega') \frac{(1 - e^{i\omega't})}{(\omega')^2} &= \lim_{|t| \rightarrow \infty} \int d\omega' \rho_{f\mathbf{k}}(\omega') \left[\frac{1 - \cos\omega't}{(\omega')^2} + i \frac{\sin\omega't}{(\omega')^2} \right] \\ &= \int d\omega' \frac{\rho_{f\mathbf{k}}(\omega')}{(\omega')^2 + t^{-2}} + i \lim_{|t| \rightarrow \infty} \int d\omega' \rho_{f\mathbf{k}}(\omega') \frac{\sin\omega't}{(\omega')^2}, \end{aligned} \quad (45)$$

where we have also made use of the equivalence of the two distributions in the long-time limit:

$$\lim_{|t| \rightarrow \infty} \frac{(1 - \cos\omega't)}{(\omega')^2} \rightarrow \lim_{|t| \rightarrow \infty} \frac{1}{(\omega')^2 + t^{-2}}.$$

Since the large t limit in (45) implies that the dominant contribution to the integral comes from the interval around $\omega' = 0$, we shall expand $\rho_{f\mathbf{k}}(\omega')$ into powers series and retain only the zeroth and first-order term in ω' . This yields

$$\lim_{|t| \rightarrow \infty} C_{f\mathbf{k}}^{\text{trans}}(t) \cong -\pi\rho_{f\mathbf{k}}(0)t - \rho'_{f\mathbf{k}}(0) \int_{E_l}^{E_u} d\omega' \frac{\omega'}{(\omega')^2 + t^{-2}} - i \left[\rho_{f\mathbf{k}}(0) \int_{E_l}^{E_u} d\omega' \frac{\sin\omega't}{(\omega')^2} + \rho'_{f\mathbf{k}}(0) \int_{E_l}^{E_u} d\omega' \frac{\sin\omega't}{\omega'} \right], \quad (46)$$

where $\rho'_{f\mathbf{k}}(\omega) = \partial\rho_{f\mathbf{k}}(\omega)/\partial\omega$, and E_u and E_l stand for the upper and lower integration boundary determined by the upper and lower band edges of $\rho_{f\mathbf{k}}(\omega')$, respectively. Thus, the expression (46) depends crucially on the width $2W$ of the conduction band, as this is the maximum energy of an e - h pair excited within this band, giving $E_u = 2W$, and the maximum recoil energy of the f -hole $2D$, giving $E_l = -2D$. Hence, the functional behavior of (46) will be governed by the ratio D/W . Quite generally, in discussing the spectral properties of $G_{\mathbf{k}}(t)$ we may distinguish two cases.

(i) *f band is infinitely narrow (infinite f-hole mass)*. In this case $D = 0$ and consequently $E_l = 0$, $\Delta_{\mathbf{k}q} = 0$, and $\rho_{f\mathbf{k}}(0) = 0$ and $\rho'_{f\mathbf{k}}(0) \neq 0$ which yields

$$\lim_{|t| \rightarrow \infty} C_{f\mathbf{k}}^{\text{trans(i)}}(t) = \rho_{f\mathbf{k}}(0) \ln(1 - iE_u t), \quad (47)$$

and leads to a power-law divergence of $N_{f\mathbf{k}}(\omega)$ at the threshold at $\omega = \bar{\epsilon}_{\mathbf{k}}$ [cf. Eq. (13) of Ref. 11]. In addition, the relaxation shift v_f given by (42) reaches a maximum value. The physical implication of the infinite f -hole mass on the spectral shape of the hole was discussed in Ref. 11.

(ii) *f band has finite width (mobile hole)*. In this case $D \neq 0$, $\Delta_{\mathbf{k}q} \neq 0$, $E_l = -2D < 0$, and

$$\begin{aligned} \lim_{|t| \rightarrow \infty} C_{f\mathbf{k}}^{\text{trans(ii)}}(t) &= \lim_{|t| \rightarrow \infty} \left[-\pi\rho_{f\mathbf{k}}(0)t - \rho'_{f\mathbf{k}}(0) \ln \left[\frac{1 + (E_u t)^2}{1 + (E_l t)^2} \right]^{1/2} - i\pi\rho'_{f\mathbf{k}}(0) \right] \\ &= -\pi\rho_{f\mathbf{k}}(0)t + \rho'_{f\mathbf{k}}(0) \ln \frac{D}{W}. \end{aligned} \quad (48)$$

Using (48) the shape of the elastic line in the f -hole spectrum is obtained from (23) and reads

$$\lim_{\omega \rightarrow \bar{\epsilon}_{\mathbf{k}}} N_{f\mathbf{k}}^{\text{elastic}}(\omega) = Z_f \frac{\Gamma_f / \pi}{(\omega - \bar{\epsilon}_{\mathbf{k}})^2 + \Gamma_f^2}, \quad (49)$$

where

$$\Gamma_f = \pi\rho_{f\mathbf{k}}(0) \quad (50)$$

is the total probability per unit time that the hole in the process of recoil will excite an electron-hole pair in the conduction band. The term

$$Z_f = \left[\frac{D}{W} \right]^{\rho'_{f\mathbf{k}}(0)}, \quad (50a)$$

gives the weight of the elastic line in the spectrum and has the appearance of an electronically induced Debye-Waller factor. With the recoil given by (40), i.e., evaluated in the local approximation, both Γ_f and Z_f are \mathbf{k} independent.

Note that in the case of infinite hole mass ($Z_f = 0$ since

$D = 0$) the no loss line has zero weight and the entire spectral weight is accumulated in the inelastic part of the spectrum, i.e., in a totally asymmetric infrared threshold divergence extending below the threshold at $\bar{\epsilon}_{\mathbf{k}}$ [cf. Ref. 11, Eq. (13)].

2. Intermediate-time behavior of $G_{\mathbf{k}}(t)$

The intermediate-time behavior of $G_{\mathbf{k}}(t)$ determines the line shape of $N_{f\mathbf{k}}(\omega)$ away from the elastic line, i.e., outside the region $|\omega - \bar{\epsilon}_{\mathbf{k}}| \leq \Gamma_f$ of the main peak. This time dependence is governed by the oscillatory factor in the integral of (44), viz., by the term

$$\int d\omega' \rho_{f\mathbf{k}}(\omega') \frac{e^{i\omega't}}{(\omega')^2}, \quad (51)$$

as all other terms contribute either to the shift v_f of the elastic line or to its weight Z_f (cf. above). Since in the present limit we are interested only in the interval of the spectral density $N_{f\mathbf{k}}(\omega)$ for which $|\omega - \bar{\epsilon}_{\mathbf{k}}| \geq \Gamma_f$, the spurious divergence $1/(\omega')^2$ in the integrand of (51) can

be healed either by using the Ansatz

$$\frac{1}{(\omega')^2} \rightarrow \frac{1}{(\omega')^2 + \Gamma_f^2}, \quad \text{for } |\omega'| < \Gamma_f \quad (52)$$

or by cutting off the ω' integration below $|\omega'| = \Gamma_f$. Both procedures lead to essentially the same result and for the sake of mathematical simplicity we choose the former one. Such a renormalization of the denominator in the integrand of (51) would also be obtained by taking into account that the initial-hole state decays through recoil since $D \neq 0$ (except when the hole is created at the upper edge of the filled f band), a feature that would also appear in higher-order cumulants in the expansion of the evolution operator (27).

To obtain the dominant spectral characteristics of $N_{f\mathbf{k}}(\omega)$ we may assume the weak-coupling limit [small effective $|V_{\mathbf{q}}|^2$, cf. Ref. 21(b)] and make use of (52) to carry out the expansion

$$\exp[C_{f\mathbf{k}}^{\text{trans}}(t)] = 1 + C_{f\mathbf{k}}^{\text{trans}}(t) + O(|V_{\mathbf{q}}|^4), \quad (53)$$

which yields, for $|\omega - \bar{\epsilon}_{\mathbf{k}}| > \Gamma_f$,

$$\begin{aligned} N_{f\mathbf{k}}^{\text{inelastic}}(\omega) &= Z_f \int_{-\infty}^{\infty} \frac{dt}{2\pi} \int d\omega' \frac{\rho_{f\mathbf{k}}(\omega')}{(\omega')^2 + \Gamma_f^2} e^{i(\omega - \bar{\epsilon}_{\mathbf{k}} + \omega')t} \\ &+ O(|V_{\mathbf{q}}|^4) \\ &= Z_f \frac{\rho_{f\mathbf{k}}(\bar{\epsilon}_{\mathbf{k}} - \omega)}{(\bar{\epsilon}_{\mathbf{k}} - \omega)^2 + \Gamma_f^2} + O(|V_{\mathbf{q}}|^4). \end{aligned} \quad (54)$$

Thus, the same functional form of $N_{f\mathbf{k}}(\omega)$ is obtained both from the long-time and the intermediate-time calculations. By combining Eqs. (49) and (54) and recalling that $\Gamma_{\mathbf{k}} = \pi\rho_{f\mathbf{k}}(0)$, we finally obtain the weak-coupling result:

$$N_{f\mathbf{k}}(\omega) = Z_f \left[\frac{\rho_{f\mathbf{k}}(\bar{\epsilon}_{\mathbf{k}} - \omega)}{(\bar{\epsilon}_{\mathbf{k}} - \omega)^2 + \Gamma^2} + O(|V_{\mathbf{q}}|^4) \right], \quad (55)$$

for the entire ω interval. However, note that Z_f appearing in (55) and defined by (50a) is not restricted to the weak-coupling approximation employed in (53) and, hence, represents the correct Debye-Waller factor for the entire spectrum. The form of the first term in the large bracket on the RHS of (55) is also known from the studies of decaying states in the radiation theory (cf. Ref. 22, p. 994).

The expression (55) for the f -hole spectral density embodies both the elastic and inelastic components of the spectrum. With the adiabatic part of the problem solved in the local approximation, $N_{f\mathbf{k}}(\omega)$ turns out \mathbf{k} independent, and its behavior is shown in Fig. 3 for the same set of parameters as used in Fig. 2. The shapes of the spectra depend crucially on the magnitude of the parameter $a = (\pi/d)/q_{\text{TF}}$, viz., on the effective strength of the interaction of the f hole with the charge-density fluctuations (electron-hole pairs) in the conduction band. In the case of a small a (weak dynamical screening) the spectrum is dominated by an asymmetric no loss (elastic) line

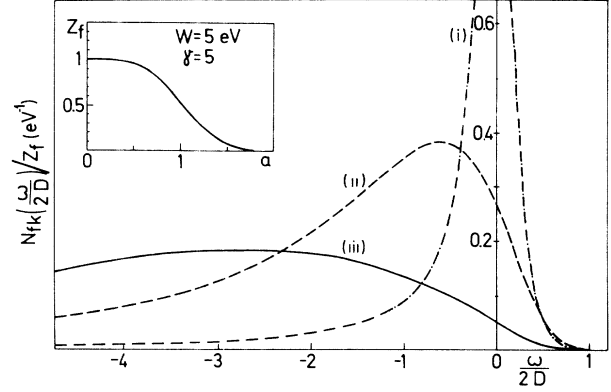


FIG. 3. The f -hole spectral density (with final-state effects included), $N_{f\mathbf{k}}(\omega)/Z_f$, plotted as a function of energy for the same values of $a = (\pi/d)/q_{\text{TF}}$ and γ as in Fig. 2. Inset: behavior of Z_f as a function of a for $\gamma = 5$ and $W = 5$ eV.

centered at $\omega = \bar{\epsilon}_{\mathbf{k}}$ (zero in Fig. 3). As a increases the probability of inelastic excitation of the conduction-band electron-hole pairs of higher energy also increases. This shifts the weight of the spectrum from the no loss line towards an inelastic side wing whose maximum now lies outside the range $2D$ of the maximum f -hole recoil energy. The same qualitative behavior of $N_{f\mathbf{k}}(\omega)$ is also obtained for other values of γ which are of the same order of magnitude (e.g., $\gamma = 10$). In all cases, however, the main spectral feature is a pronounced asymmetry towards the higher-binding-energy side, which is a consequence of a rather singular coupling of the heavy f hole to the conduction-band e - h pairs near the Fermi level. This becomes particularly important in the limit of infinitely heavy hole [case (i) discussed above with $D = 0$], in which case the f spectrum would acquire a singular shape with zero weight of the elastic line ($Z_f = 0$), and an integrable divergence for the inelastic side band extending below $\bar{\epsilon}_{\mathbf{k}}$ (cf. Ref. 11).

The inset in Fig. (3) shows the dependence of the Debye-Waller factor Z_f given by Eq. (50a) as a function of the effective strength of the interaction a , for $D = 1$ eV and $W = 5$ eV (i.e., $\gamma = 5$). The behavior of Z_f demonstrates clearly that in the limit $a > 1$, which implies efficient screening or strong coupling of the f hole to the conduction-band charge-density fluctuations, the weight of the elastic line is strongly reduced, whence the majority of the spectral weight appears in the inelastic side band of the spectrum $N_{f\mathbf{k}}(\omega)$ [see curve (iii) in Fig. 3].

The shape function $N_{f\mathbf{k}}^{\text{trans}}(\omega)$ [Eq. (36)] is obtained from (55) by setting $\bar{\epsilon}_{\mathbf{k}} = 0$, i.e.,

$$N_{f\mathbf{k}}(\omega) = N_{f\mathbf{k}}^{\text{trans}}(\omega - \bar{\epsilon}_{\mathbf{k}}). \quad (56)$$

Using this, we find that the overall effect of such a shape function on the measured (integrated) spectra may readily be deduced from Eq. (35). Employing the results of Sec. II we may assume a simple density of states within the f band, viz.,

$$N_{f\mathbf{k}}^a(\omega') = \bar{\alpha}_{\mathbf{k}} \delta(\omega' - \bar{\epsilon}_{\mathbf{k}}) \quad \text{for } \epsilon_f - D \leq \bar{\epsilon}_{\mathbf{k}} \leq \epsilon_f + D, \quad (57)$$

wherefrom we obtain:

$$N_f(\omega) = \sum_{\mathbf{k}} \bar{\alpha}_{\mathbf{k}}^- N_{f\mathbf{k}}^{\text{trans}}(\omega - \bar{\epsilon}_{\mathbf{k}} - v_f) \approx \int d\epsilon N_f^a(\epsilon) N_f^{\text{trans}}(\omega - \epsilon - v_f). \quad (58)$$

Here, $N_f^a(\epsilon)$ is the ‘‘adiabatic’’ or the initial density of states in the f band as obtained from the diagonalization of H_a of Eq. (1) and shown in Fig. 1, and $N_f^{\text{trans}}(\omega - \epsilon - v_f)$ is the \mathbf{k} -independent shape function obtained from (56), which now includes the relaxation shift v_f as a typical final-state feature.

Equation (58) gives a nice example of how the measured XPS spectrum of an occupied f band of a heavy-fermion system appears as a convolution of the adiabatic or initial-state band structure, expressed here through N_f^a , and the nonadiabatic, final-state effects embodied in the shape function N_f^{trans} .

In the limit of weak screening (small a), the width $2D$ of the occupied f band will be much larger than the width $2\Gamma_f$ of $N_f^{\text{trans}}(\omega)$ [cf. curve (i) in Fig. 3]. In this case $N_f^{\text{trans}}(\omega)$ (which is normalized to unity) may be approximated by $\delta(\omega - \epsilon - v_f)$, yielding for small a :

$$N_f(\omega) \cong N_f^a(\omega - v_f). \quad (59)$$

Hence, in the weak-screening limit the XPS spectrum $N_f(\omega)$ will be shifted upwards towards ϵ_F by v_f , but will retain the overall shape determined by the initial-state effects (except for some asymmetry at the lower band edge).

In the opposite limit of strong screening (a large), the width of N_f^{trans} will largely exceed the initial-state width $2D$ of the f band. In this situation N_f^a , which is also normalized to unity, may be approximated by $\delta(\epsilon - \epsilon_f)$, now yielding for large a :

$$N_f(\omega) = N_f^{\text{trans}}(\omega - \epsilon_f - v_f). \quad (60)$$

In this case the XPS spectrum is dominated by the final-state effects both through the upward relaxation shift v_f and the pronounced asymmetric shape tailing towards higher binding energies. The initial-state structure enters here only through the position ϵ_f of the center of the occupied f band.

In both limits of the XPS line shapes discussed [viz., (59) and (60)], the upward relaxation shift and the overall asymmetry of the f peak would persist, signifying an interplay between the initial- and final-state effects in photoemission from the occupied narrow f bands lying well below ϵ_F . This feature becomes more pronounced as the efficiency of screening of the f hole brought about by the conduction-band electrons is enhanced (i.e., as q_{TF} is lowered). These facts should be taken into account when interpreting the XPS and other experimental data on the f -band electronic structure of strongly correlated fermion systems.

The above conclusions apply equally well to the inverse photoemission (BIS) spectra of the unoccupied part of the f band lying above ϵ_F , in which case all the final-state features are reflected across ϵ_F . Thus, by applying the time reversal to Eqs. (35)–(54), one finds (cf. Refs. 11 and

23) that the BIS spectra of unoccupied f states exhibit *downward* relaxation shift and *asymmetric* broadening towards *higher* energies.

IV. DISCUSSION

Before applying the results of the preceding sections to the electronic spectra of actinide intermetallic compounds we recall some of the simplifying assumptions made in the course of our derivations and summarize briefly the experimental status in the field.

Our treatment is based on the nondegenerate periodic Anderson model in which the correlated electrons are delocalized through the hybridization with the neighboring ligands, like in actinide intermetallics. Thus, with the actual orbital degeneracy and the spin-orbit coupling being neglected, the occupied $5f$ band of actinides is reduced to an effective ‘‘one-electron’’ band which accommodates most of the f charge. Its width, $2D$, is found not to be very different from the values given by the local-density approximation (LDA), but, in contrast to the results obtained by the LDA, its center is displaced away from ϵ_F by $U/2$, due to the effects of local correlation, $U \gg D$. Within our full many-body treatment the effect of correlation U also gives rise to the formation of a narrow ‘‘heavy-particle band’’ right at ϵ_F (cf. Ref. 6). However, the contribution of these ‘‘heavy states’’ to the overall charge neutrality of the system is so small that it can be neglected. Hence, only the states in the effective ‘‘one-electron’’ band are assumed to be probed in XPS (or BIS) experiments. Furthermore, we assume that the time scale characterizing the charge redistribution in uncorrelated s, p, d bands is so short that the transient effects associated with XPS (or BIS) can be treated independently from the ‘‘Kondo effect.’’

As regards the experimental data, the characteristic feature of the $5f$ -derived part of the uranium XPS spectra is the presence of a single, asymmetrically broadened peak centered a few eV below ϵ_F . In heavy-fermion compounds such as UBe_{13} , UAl_2 , or UPt_3 ,^{24,25} the peak overlaps the Fermi level but much more weight is found in a broader interval around ϵ_F than could be expected from the narrow ‘‘heavy-particle band,’’ whose existence is otherwise indicated by the equilibrium data. If the distance between the center of the f peak and ϵ_F , as observed in XPS, would be taken as a measure of the f - f correlation U , the derived Kondo temperature and the associated width of the ‘‘heavy-particle band’’ would again turn out to be inconsistent with low-temperature thermodynamics. Moreover, the overall width of the measured $5f$ peak greatly exceeds the theoretical predictions based on the independent-electron approximation.^{26,27} The puzzling spectra are also obtained for the $\text{Y}_x\text{U}_{1-x}\text{Pd}_3$ compounds, in which the $5f$ states are assumed to be localized.⁴ Here, the f -derived peak is well separated from ϵ_F but the separation decreases with the addition of Y impurities. Since the dilution of uranium, if anything, should increase the local character of the f states, it seems that the position of the $5f$ peak in actinide intermetallics is not related only to the f - f correlation. Thus, we would like to understand the following

observations made for uranium-based heavy-fermion intermetallics: (i) the excess width of the experimental $5f$ XPS spectra relative to the one-electron description, (ii) the proximity of these broad spectra to ε_F in systems that exhibit large mass enhancement, and (iii) the absence of additional spectral weight which would give the spectroscopic evidence for the Kondo peak. In UPd₃ compounds, in which the f electrons are assumed to be localized,^{28,29} we would also like to understand the unusual shifting of the spectra upon doping.

Having in mind the simplifications made in order to carry out the calculations, we can only attempt a qualitative comparison between the theory and the experimental data. The question of our prime interest here is whether the observations mentioned above, together with the thermodynamic and transport data, could be interpreted and understood within the framework of the periodic Anderson model.

Let us focus our attention on the position of the relaxed peak as given by Eq. (43). The center of the occupied f band of width $2D$ lies at $\varepsilon_f = -U/2$, well below ε_F (cf. Fig. 1), but the observed energy $\bar{\varepsilon}_f$ of the f states will be shifted upward by the final-state relaxation effects [cf. Eq. (42)] to a value

$$\bar{\varepsilon}_f = \varepsilon_f + v_f, \quad (61)$$

i.e., closer to ε_F by the amount v_f given by Eq. (42). The magnitude of v_f can be estimated only roughly because its explicit calculation would require the knowledge of the full response function of the systems studied, and these are currently not available. In making the estimate we notice first that the final-state relaxation effects of localized core levels of some $3d$ metals have been calculated and found^{30,31} to vary between 3 and 6 eV. As regards the uranium $5f$ states, the additional change of the magnitude of the relaxation shift due to the delocalization is an effect of the order $v_{\text{loc}}(D/\Omega)$, where v_{loc} is a shift of an "equivalent" localized $5f$ level and Ω is the characteristic excitation energy of the electronic response (typically the plasmon energy, which exceeds 10–20 eV in most metals and intermetallics), and therefore the main effect comes from v_{loc} . Thus, from the arguments of perfect screening in metals, we should expect the relaxation shifts of about 3–6 eV in our problem as well. This implies that although the ground-state position of the center of the f band may lie well below ε_F (cf. Fig. 1), in XPS the corresponding peak will show up much closer to the Fermi level, the actual position depending on the magnitude of $U/2 - v_f$. Thus, in the uranium-based heavy-fermion intermetallics, we identify the f -derived XPS peak as originating from the one-electron density of the occupied f states centered around ε_f in the ground state (charge equilibrium state), and shifted upwards by screening effects in the relaxed final ionized state.

Such an identification is further supported by the comparison between the shape of the observed XPS spectra and the calculated spectral lines displayed in Fig. 3. The characteristic feature of measured spectra is their width and asymmetry with a tail extending towards negative energies (i.e., away from ε_F). This feature is interpreted in

our model as originating from final-state dynamic screening of the f hole whose sudden appearance in photoemission gives rise to a nonadiabatic excitations of charge-density fluctuations within the conduction band. As a consequence, the hole recoils and the energy of the photoemitted electron is reduced by the amount of the excitation energy of the charge-density fluctuation. Both processes contribute to the observed peak width $\Gamma_f > 2D$ [Eq. (50a)], and the latter process gives rise to the peak asymmetry. A mere inspection of the experimental spectra of Ref. 4 and the comparison with our Fig. 3 shows that the experimental XPS f -line shapes are modeled quite well by our curves (i) and (ii). The latter were calculated with the choice of the free-electron parameter $q_{\text{TF}} = q_{\text{TF}}(r_s)$ for which the free-electron parameter r_s lies in the range $2 < r_s < 3$, and this spans the interval of realistic r_s values for a large number of metals. If the low-energy part of the XPS line is too close to ε_F , the small additional feature that might be expected due to the Kondo resonance will not be observed.

As regards the UPd₃ and similar systems with localized f states, we believe that the addition of impurities could change to some extent only the screening properties of the conduction electrons, which may manifest itself in the position and the shape of the XPS line upon doping. On the other hand, the unperturbed "one-electron" f band is insensitive to the addition of impurities.

We also remark that in the systems where the f -derived XPS line remains to be split off from the Fermi level, as the consequence of different conduction electrons screening properties, the Kondo resonance could be observed at low enough temperatures, $T < T_K$, provided the experimental resolution is large enough. We believe this is the situation one encounters in cerium-based heavy-fermion intermetallics,⁴ but even there the width and position of the experimental XPS spectra could not be simply related to the parameters of the Anderson Hamiltonian so as to yield a quantitative agreement between the model parameters deduced from the low-energy and high-energy experiments, unless the final-state effects are taken into account.

To summarize, our model, which incorporates the band characteristics as an initial-state effect and the relaxation shift and the line shapes as the final-state effects, enables us to make a proper assignment and give the interpretation of the XPS spectra as an interplay between the ground-state properties of the system and the dynamic screening effects characteristic of photoemission from metals. The present assignment of the peaks allows us to remove the conceptual difficulty in understanding the data acquired independently from thermodynamic and spectroscopic measurements of actinide systems within a unified framework.

ACKNOWLEDGMENTS

This work was supported in part by SIZ znanosti SRH (Yugoslavia), NSF Grant No. JF 798, DOE Grant No. JF 817-31, and German-Yugoslav project No. 32.2.A.F. "Oberflächenphysik."

- *Permanent address: Institute of Physics of the University of Zagreb, 41001 Zagreb, P.O.B. 304, Yugoslavia.
- ¹P. A. Lee, T. M. Rice, J. W. Serene, L. J. Sham, and J. W. Wilkins, *Comments Condens. Mat. Phys.* **12**, 99 (1986).
- ²K. Yamada and K. Yosida, in *Electron Correlation and Magnetism in Narrow Band Systems*, Vol. 29 of *Springer Series of Solid State Physics*, edited by T. Moriya (Springer, Berlin, 1981).
- ³P. Fulde, J. Keller, and G. Zwicknagl, in *Solid State Physics*, edited by F. Seitz, D. Turnbull, and H. Ehrenreich (Academic, New York, 1988).
- ⁴J. W. Allen, *J. Magn. Magn. Mater.* **76&77**, 324 (1988).
- ⁵K. Yamada and K. Yosida, *Prog. Theor. Phys.* **76**, 621 (1986).
- ⁶V. Zlatić, S. K. Ghatak, and K. H. Bennemann, *Phys. Rev. Lett.* **57**, 1263 (1986); K. Okada, Y. Yamada, and K. Yosida, *Prog. Theor. Phys.* **77**, 1297 (1987).
- ⁷K. Yamada and K. Yosida, *Prog. Theor. Phys. Suppl.* **46**, 244 (1970).
- ⁸V. Zlatić, P. Entel, B. Horvatić, and D. Schulz, *Int. J. Mod. Phys.* **1**, 811 (1988); B. Horvatić and V. Zlatić (unpublished).
- ⁹V. Zlatić, A. A. Aligia, and D. Schulz, *J. Magn. Magn. Mater.* **76&77**, 70 (1988).
- ¹⁰H. Schweitzer and G. Czycholl, *J. Magn. Magn. Mater.* **76&77**, 77 (1988).
- ¹¹V. Zlatić, B. Gumhalter, and S. K. Ghatak, *Phys. Rev. B* **35**, 902 (1987).
- ¹²B. Gumhalter, *Prog. Surf. Sci.* **15**, 1 (1984).
- ¹³J. B. Pendry, *Phys. Rev. Lett.* **45**, 1356 (1980).
- ¹⁴C.-O. Almbladh and L. Hedin, in *Handbook on Synchrotron Radiation*, edited by E. E. Koch (North-Holland, Amsterdam, 1983), Vol. 1, p. 611.
- ¹⁵E. Müller-Hartmann, T. V. Ramakrishnan, and G. Toulouse, *Phys. Rev. B* **3**, 1102 (1971).
- Phys. Rev. B* **3**, 1102 (1971).
- ¹⁶S. Doniach, *Phys. Rev. B* **2**, 3898 (1970).
- ¹⁷Ž. Crljen and B. Gumhalter, *Phys. Rev. B* **29**, 6600 (1984).
- ¹⁸D. Lovrić and B. Gumhalter, *Phys. Rev. B* **38**, 10 323 (1988).
- ¹⁹D. C. Langreth, *Phys. Rev. B* **1**, 471 (1971).
- ²⁰G. Mahan, *Many Particle Physics* (Plenum, New York, 1981), p. 305.
- ²¹(a) Ph. Nozieres and C. T. De Dominicis, *Phys. Rev.* **178**, 1097 (1969); (b) J. Gavoret, Ph. Nozieres, B. Roulet, and M. Combescot, *J. Phys. (Paris)* **30**, 987 (1969).
- ²²A. Messiah, *Quantum Mechanics* (North-Holland, Amsterdam, 1965), Vol. 2.
- ²³B. Gumhalter, *Surf. Sci.* **157**, L355 (1985).
- ²⁴E. Wuilloud, Y. Baer, H. R. Ott, Z. Fisk, and J. L. Smith, *Phys. Rev. B* **29**, 5228 (1984); J. W. Allen, S.-J. Oh, L. E. Cox, W. P. Ellis, M. S. Wire, Z. Fisk, J. L. Smith, B. B. Pate, I. Lindau, and A. J. Arko, *Phys. Rev. Lett.* **54**, 2635 (1985).
- ²⁵A. J. Arko, C. G. Olson, D. M. Wieliczka, Z. Fisk, and J. L. Smith, *Phys. Rev. Lett.* **53**, 2050 (1984).
- ²⁶P. Marksteiner, P. Weinberger, R. C. Albers, A. M. Boring, and G. Schadler, *Phys. Rev. B* **34**, 6730 (1986).
- ²⁷A. M. Boring, R. C. Albers, G. Schadler, P. Marksteiner, and P. Weinberger, *Phys. Rev. B* **35**, 2447 (1987).
- ²⁸Y. Baer, in *Handbook on the Physics and Chemistry of the Actinides*, edited by J. Freeman and G. H. Lander (North-Holland, Amsterdam, 1984), Vol. 1.
- ²⁹A. J. Arko, D. D. Koelling, B. D. Dunlap, and A. W. Mitchell, *J. Appl. Phys.* **63**, 3680 (1988).
- ³⁰F. F. Egelhoff, Jr., *Surf. Sci. Rep.* **6**, 253 (1987).
- ³¹A. R. Williams and N. D. Lang, *Phys. Rev. Lett.* **40**, 954 (1978).